

# Discharge Stabilization Method of an Anode Layer Type Hall Thruster by Non-uniform Propellant Flow

IEPC-2009-148

*Presented at the 31st International Electric Propulsion Conference,  
University of Michigan • Ann Arbor, Michigan • USA  
September 20 – 24, 2009*

Yasuhiro Fukushima<sup>1</sup>, Shigeru Yokota<sup>2</sup>, Daosike Takahashi<sup>3</sup>, Kentaro Hara<sup>4</sup>, Shinatora Cho<sup>5</sup>,  
Kimiya Komurasaki<sup>6</sup>, and Yoshihiro Arakawa<sup>7</sup>  
*The University of Tokyo, Tokyo, Japan.*

Discharge current oscillation at the frequency of 10-100 kHz causes serious problems in using an anode layer type Hall thruster in space. As a novel approach to the oscillation reduction, azimuthally nonuniform propellant flows were created in an acceleration channel. As a result, the small-amplitude oscillation region became significantly wide. Although the thrust efficiency decreased in exchange due to increase in electron current from the channel exit, the tradeoff curve between oscillation amplitude and thrust efficiency was improved by introduction of a new parameter “differential flow rate.” In this study, the small-amplitude oscillation region with 42-64 mT width and the thrust efficiency 39%, which is roughly equivalent to the magnetic layer type thrusters with the same channel diameters, was achieved.

## Nomenclature

$B$	= magnetic flux density
$E$	= electric field
$e$	= elementary electric charge
$F$	= thrust
$I_b$	= ion beam current
$I_d$	= discharge current
$I_e$	= electron backflow current
$I_g$	= guard ring current
$k_B$	= Boltzmann constant
$\dot{m}_{\text{dif}}$	= differential of mass flow rate
$\dot{m}_{\text{tot}}$	= total mass flow rate
$n_e$	= electron number density
$r$	= radial component of cylindrical coordinate
$T_e$	= electron temperature
$V_d$	= discharge voltage
$v_e$	= electron velocity
$z$	= axial component of cylindrical coordinate

---

<sup>1</sup> Graduate Student, Department of Aeronautics and Astronautics.

<sup>2</sup> Assistant Professor, Department of Aeronautics and Astronautics.

<sup>3</sup> Graduate Student, Department of Aeronautics and Astronautics.

<sup>4</sup> Graduate Student, Department of Aeronautics and Astronautics.

<sup>5</sup> Graduate Student, Department of Aeronautics and Astronautics.

<sup>6</sup> Professor, Department of Advanced Energy.

<sup>7</sup> Professor, Department of Aeronautics and Astronautics.

- $\Delta$  = oscillation amplitude
- $\phi$  = electric potential
- $\eta_t$  = thrust efficiency
- $\nu_{en}$  = electron – neutral collision frequency
- $\theta$  = azimuthal component of cylindrical coordinate
- $\tau$  = measuring time of discharge current

**suffix**

- A = high plasma density region
- B = low plasma density region

## I. Introduction

A Hall thruster<sup>1,2</sup> is one of the most attractive propulsion devices for near-Earth missions because of its high thrust efficiency at the specific impulse in the range of 1,000-3,000 s. In general, Hall thrusters are categorized into the magnetic layer type and the anode layer type.<sup>3</sup> The former type has been used in many missions while the latter type still remains under development. The anode layer type has several advantages such as higher thrust efficiency, compactness and high erosion resistance.<sup>4,5</sup> However, its operation tends to be unstable due to the discharge current oscillation and to be limited in a narrow range of operation parameters. This is one of the most serious problems in using it as a reliable satellite engine.

Until now, several studies have been conducted to stabilize the oscillation.<sup>6-10</sup> In general, a hollow anode<sup>5-7</sup> is used to stabilize the oscillation. However, even if the hollow anode is used, the stable operation region is limited to a narrow range.

The discharge characteristic of a Hall thruster highly depends on the magnetic field  $B$ .<sup>6-9</sup> Figure 1 shows the average discharge current  $I_d$ , the oscillation amplitude  $\Delta$ , the thrust efficiency  $\eta_t$  and the thrust  $F$  as a function of  $B$ . Here,  $\Delta$  and  $\eta_t$  are defined as

$$\Delta \equiv \frac{1}{I_d} \sqrt{\frac{\int_0^\tau (I_d - \bar{I}_d)^2 dt}{\tau}} \quad \left( \bar{I}_d \equiv \frac{\int_0^\tau I_d dt}{\tau} \right), \quad (1)$$

$$\eta_t \equiv \frac{F^2}{2\dot{m}_{tot} I_d V_d} \quad (2)$$

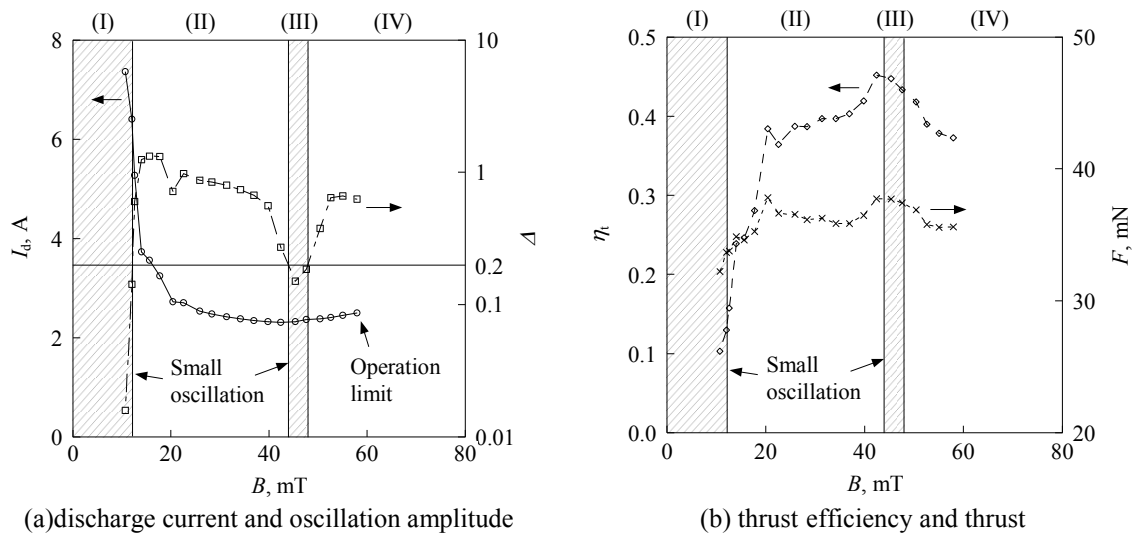


**Figure 1. Thrust performance as a function of magnetic flux density.**  $\dot{m}_{tot} = 2.73 \text{ mg/s}$ ,  $V_d = 250 \text{ V}$ , The hollow anode width is 3mm.

In general,  $\Delta < 0.2$  is satisfied in the practical use of a magnetic-layer-type Hall thruster.<sup>11,12</sup> In this study, we define that the discharge oscillation is small when  $\Delta$  is smaller than 0.2. As shown in Fig. 1,  $\Delta < 0.2$  is satisfied in range (I) and (III). However, the operation in the range (I) is not desirable because  $\eta_t$  is low due to the large  $I_d$ . On the other hand,  $\eta_t$  in range (III) is high, however the range is narrow. The purpose of this study is to extend this narrow stable operation range (III). In order to realize it, we focused on an oscillation reduction effect of azimuthally nonuniform propellant flow rate. This effect was found in the study of the thrust vector control using biased propellant feeding.<sup>13</sup> In this study, we applied this method to discharge stabilization of an anode layer type Hall thruster.

## II. Experimental Setup

### A. Experimental Setup

#### 1. Hall Thruster

An anode layer type Hall thruster developed at the University of Tokyo was used in this study (Fig. 2). Its inner and outer diameters of acceleration channel are 48 and 62 mm, respectively. The guard rings are made of stainless steel and their potential was kept same as the cathode. A hollow anode with the hollow width of 3 mm and anode-tip-to-thruster-exit distance of 3 mm was used. This configuration is the most effective one for discharge stabilization according to the past study.<sup>14</sup> Magnetic field in the acceleration channel was generated by a solenoidal coil on the thruster's central axis. The coil was protected against overheating by a water cooling system. Hollow cathode was used and xenon gas was supplied to it at 0.27 mg/s. Figure 3 shows a plenum chamber divided into four rooms. Xenon gas was supplied to each room through two pairs of two ports on the back surface of the thruster. Xenon flow rate through each port was independently controlled by two mass flow controllers.

#### 2. Vacuum Chamber

This experiment was conducted in the vacuum chamber whose diameter and length are 2.0 and 3.0 m, respectively. The pumping system comprises four pumps: a diffusion pump (37000 l/s), a mechanical booster pump (10000 m<sup>3</sup>/h) and two rotary pumps (15000 l/min). The background pressure was kept under  $3.8 \times 10^{-3}$  Pa.

#### 3. Thrust Stand

The thrust vector was measured by using a two-axis dual pendulum thrust stand.<sup>13</sup> This thrust stand has two pendulums and four arms for each pendulum. All joints consist of knife-edges. The supporting points with two orthogonal knife-edges enable pendulums to move in the two directions: axial and transverse direction of a thruster. A thruster and sensor targets are mounted on the inner pendulum and two displacement sensors are set on the outer pendulum. The thermal influence from a Hall thruster plume is cancelled out by those pendulums. According to the thrust calibration by weights, measurement errors were less than 0.25 mN in the axial direction and 0.09 mN in the transverse direction.

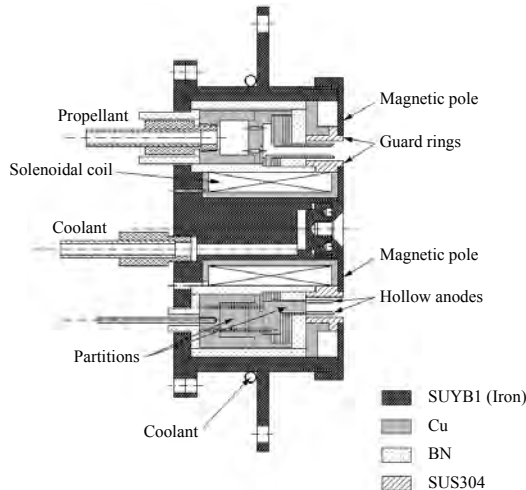


**Figure 2. Cross section of the anode layer type Hall thruster developed in the University of Tokyo.**

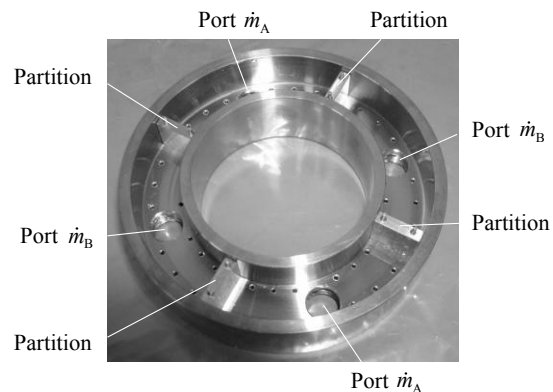


**Figure 3. A segmented plenum chamber**

#### 4. Discharge Current Measurement System

Figure 4 shows a schematic diagram of measurement system. In order to measure  $I_d$ ,  $0.5 \Omega$  metal-film resistor was inserted between anode and discharge power supply. The voltage between its both ends was measured by a digital oscilloscope at the sampling rate of 10 MHz.  $\Delta$  was deduced from  $I_d$  histories measured in 5 ms.

#### B. Measurement Method

In order to investigate the influence of azimuthally nonuniform propellant flow rate on discharge characteristics, the normalized differential mass flow rate  $\dot{m}_{\text{dif}} / \dot{m}_{\text{tot}} (= (\dot{m}_A - \dot{m}_B) / (\dot{m}_A + \dot{m}_B))$  was changed from 0.0 to 1.0 and the variation of  $I_d$ ,  $I_b$ ,  $I_g$  and  $F$  with  $B$  was measured. and  $V_d$  were kept at 1.96 mg/s and 250 V, respectively. From  $I_d$  and  $F$ ,  $\Delta$  and  $\eta_t$  were calculated.  $I_c (= I_d - I_b - I_g)$  is also calculated using the data. Figure 5 is a picture of an operation in the case of  $\dot{m}_{\text{dif}} / \dot{m}_{\text{tot}} = 1.0$ .

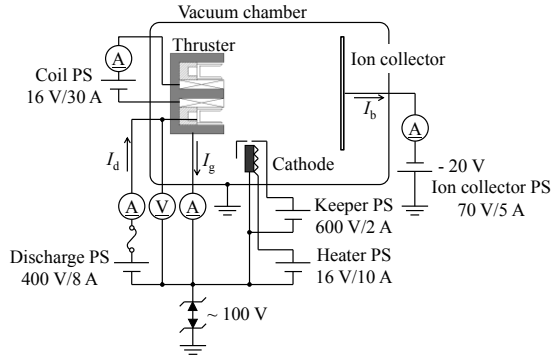


Figure 4. Schematic of the electric circuits.

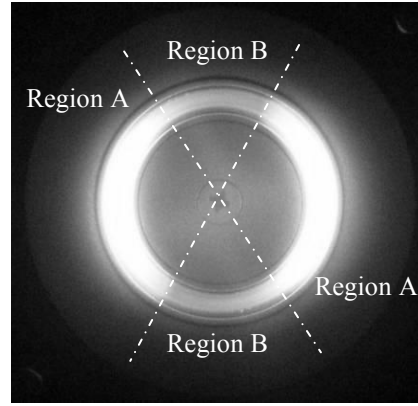


Figure 5. A picture of operation at  $\dot{m}_{\text{dif}} / \dot{m}_{\text{tot}} = 1.0$

### III. Result and Discussion

#### A. Discharge Stabilizing Effect and Thrust Efficiency

Figure 6 shows influence of  $\dot{m}_{\text{dif}} / \dot{m}_{\text{tot}}$  on  $\Delta$  as a function of  $B$ . As  $\dot{m}_{\text{dif}} / \dot{m}_{\text{tot}}$  increased, the stable operation range became wider. When  $\dot{m}_{\text{dif}} / \dot{m}_{\text{tot}} < 0.3$ ,  $\Delta$  decreased in the high  $B$  range (40 mT ~), while when  $\dot{m}_{\text{dif}} / \dot{m}_{\text{tot}}$  exceeded 0.3,  $\Delta$  decreased in the lower  $B$  range (~ 40 mT). When  $\dot{m}_{\text{dif}} / \dot{m}_{\text{tot}} = 1.0$ ,  $\Delta < 0.2$  was satisfied in all of the  $B$  range. Figure 7 shows the stable operation ( $\Delta < 0.2$ ) range of  $B$  as a function of  $\dot{m}_{\text{dif}} / \dot{m}_{\text{tot}}$ . The stable operation range become wider with the increase of  $\dot{m}_{\text{dif}} / \dot{m}_{\text{tot}}$ .

On the other hand,  $\eta_t$  decreased with increasing  $\dot{m}_{\text{dif}} / \dot{m}_{\text{tot}}$  as shown in Fig. 8; the maximum value of  $\eta_t$  fell from 0.45 to 0.18 as  $\dot{m}_{\text{dif}} / \dot{m}_{\text{tot}}$  increased from 0.0 to 1.0. Figure 9 and 10 show variation of  $I_d$  and  $F$  with  $\dot{m}_{\text{dif}} / \dot{m}_{\text{tot}}$ . As  $\dot{m}_{\text{dif}} / \dot{m}_{\text{tot}}$  increased,  $I_d$  increased while  $F$  varied only slightly. This indicates that the increase of  $I_d$  causes the decrease of  $\eta_t$ .

By introduction of the new parameter  $\dot{m}_{\text{dif}} / \dot{m}_{\text{tot}}$ , the discharge stabilization was achieved in exchange for the decrease of  $\eta_t$ . The relation between  $\eta_t$  and  $\Delta$  is summarized in Fig. 11. When the propellant is fed uniformly, the trade-off between  $\eta_t$  and  $\Delta$  is denoted by the solid line with open circles. On the other hand, when  $\dot{m}_{\text{dif}} / \dot{m}_{\text{tot}}$  is introduced as an operation parameter, the tradeoff shifts to the lower  $\Delta$  direction. Table 1 shows the thrust performance at the maximum  $\eta_t$  point in the small oscillation region and the width of the small oscillation region. The width expanded in exchange for the decrease of  $\eta_t$ .

#### B. Thruster Performance

The thrust performances of typical Hall thrusters are tabulated on Table 2. According to this data, the performance of our Hall thruster in the case of  $\dot{m}_{\text{dif}} / \dot{m}_{\text{tot}} = 0.1$  was almost equivalent to that of magnetic-layer-type Hall thruster

with the same channel diameter. This means that even if  $\eta_t$  decreases using this method, it is possible to keep its performance to the level of a magnetic layer type Hall thruster with the same channel diameter. In general, an anode layer type Hall thruster has longer life time than a magnetic-layer-type Hall thruster. Therefore, this method can contribute to extend the life time of a Hall thruster. Moreover, D-55 achieves  $\eta_t=0.60$  while  $\eta_t$  of the anode-layer-type Hall thruster used in this study is 0.45. Therefore, further high thrust efficiency can be expected in the future.

### C. Electron Current

Figure 12 shows the variation of  $I_e$  with  $\dot{m}_{dif}/\dot{m}_{tot}$ . As shown in this figure,  $I_e$  increased with  $\dot{m}_{dif}/\dot{m}_{tot}$ . This was a reason that  $I_d$  was increased as mentioned above. The increase of  $I_e$  appears to be caused by the following two effects.

First is the shift of the transition point at which point electron diffusion changed from the classical diffusion to the anomalous diffusion.<sup>6,17,18</sup> As shown Fig 12, the transition point shifted to the lower  $B$  side as  $\dot{m}_{dif}/\dot{m}_{tot}$  increased. Due to the shift,  $I_e$  in the low  $B$  range increases. The anomalous diffusion is mainly caused by the fluctuation in the azimuthal direction at the frequency of 1 ~ 100 MHz because the interaction between wall and plasma is negligible in the anode-layer-type Hall thruster. Therefore, the nonuniform mass flow rate probably induces the fluctuation in the azimuthal direction in low  $B$  range.

Second is the increase of the offset current  $I_0$  which is independent of  $B$ . The offset current was obtained from the  $I_e$  curve in the anomalous diffusion range, which is fitted with a curve give by  $c/B+I_0$ . Here,  $c$  denotes a constant which is independent of  $B$ . As shown in Fig. 12,  $I_0$  increased with  $\dot{m}_{dif}/\dot{m}_{tot}$ . The increase can be explained as follow.<sup>19</sup>

When the propellant is fed nonuniformly, the plasma number density has a distribution in  $\theta$  direction in the discharge channel of the Hall thruster, as shown in Fig. 13. Because the Hall current density is much larger than electron current density in  $z$  direction, the  $v_{e\theta,A} < v_{e\theta,B}$  must be satisfied in the case of  $n_{e,A} > n_{e,B}$ . Here,  $v_{e\theta}$  is given by

$$v_{e\theta} = -\frac{m_e v_{en}}{eB^2} \left[ E_\theta + \frac{\partial}{r\partial\theta}(n_e k_B T_e) \right] + \frac{1}{B} \left[ E_z + \frac{\partial}{\partial z}(n_e k_B T_e) \right]. \quad (3)$$

The third and fourth term in the right hand side represents the Hall current in  $\theta$  direction. In order to satisfy  $v_{e\theta,A} < v_{e\theta,B}$ ,  $E_\theta$  must be induced in  $+\theta$  direction in the high density region A and in  $-\theta$  direction in the low density region B. The cross field of  $E_\theta$  and  $B_r$  increases  $v_{ez}$  in region A while decreases in region B. As a result,  $I_e$ , which is the integral of the electron current density over  $\theta$ , increases. Here,  $E_\theta$  also increases with increasing  $\dot{m}_{dif}/\dot{m}_{tot}$  because of increase of  $v_{e\theta,B}/v_{e\theta,A}$ . In addition,  $E_\theta$  is almost proportional to  $1/B$  because the first and the second term, and the third and the fourth term of the Eq. (3) are proportional to  $1/B^2$  and  $1/B$ , respectively. Because the variation of the electron velocity in the axial direction is  $E_\theta/B$ ,  $I_0$ , which is independent of  $B$ , is induced.

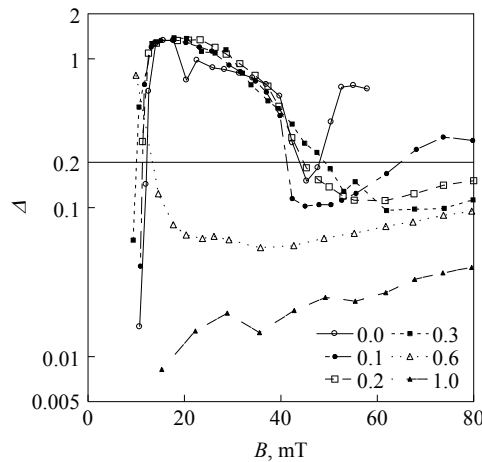


**Figure 6. Oscillation amplitude.**  $\dot{m}_{tot} = 2.73$  mg/s,  $V_d = 250$  V

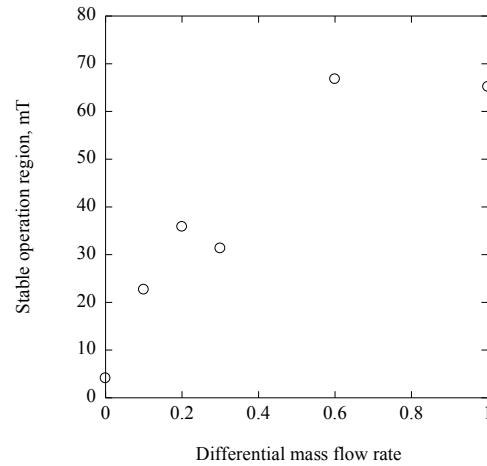


**Figure 7. Oscillation amplitude.**  $\dot{m}_{tot} = 2.73$  mg/s,  $V_d = 250$  V

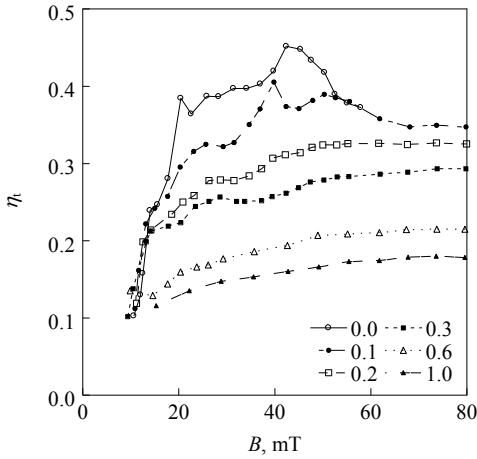


Figure 8. Thrust efficiency.  $\dot{m}_{tot} = 2.73 \text{ mg/s}$ ,  $V_d = 250 \text{ V}$ .

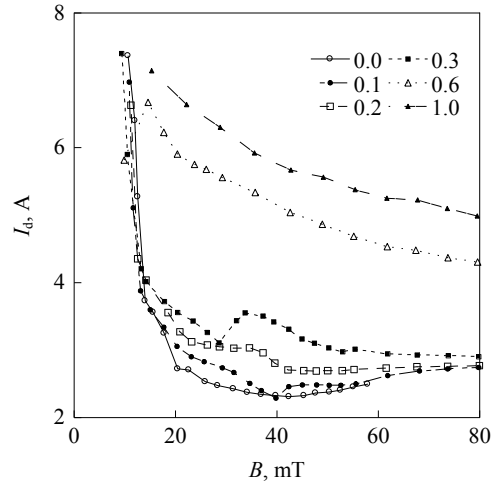


Figure 9. Discharge current.  $\dot{m}_{tot} = 2.73 \text{ mg/s}$ ,  $V_d = 250 \text{ V}$ .

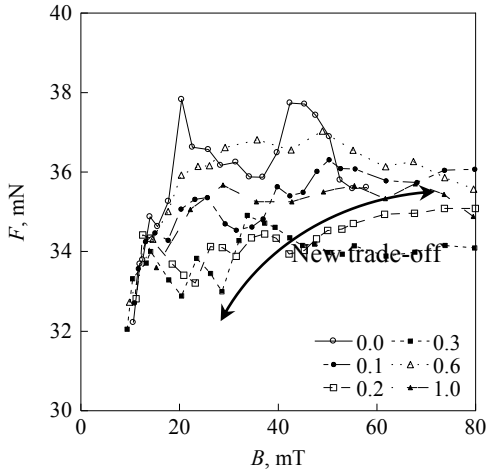


Figure 10. Thrust.  $\dot{m}_{tot} = 2.73 \text{ mg/s}$ ,  $V_d = 250 \text{ V}$ .

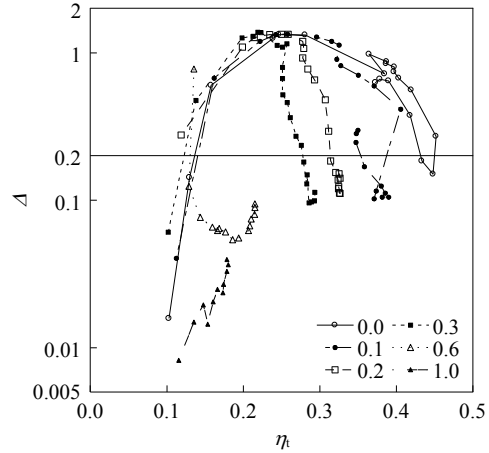


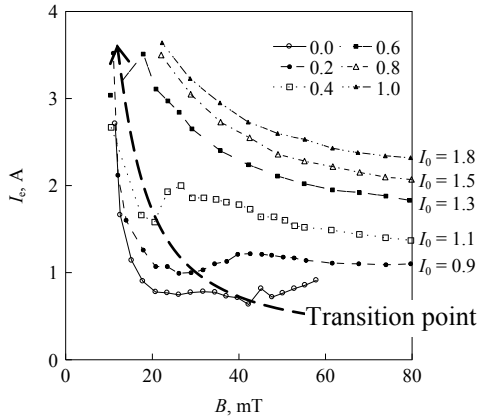
Figure 11. Discharge current.  $\dot{m}_{tot} = 2.73 \text{ mg/s}$ ,  $V_d = 250 \text{ V}$ .

Table 1 Thrust performance at the maximum  $\eta_t$  point in the small oscillation region and the width of the small oscillation region

Differential mass flow rate	0.0	0.1	0.2
Input power, W	580	620	690
Thrust, mN	38	36	35
Specific impulse, s	1400	1400	1300
Thrust efficiency	0.45	0.39	0.33
Stable operation range width, mT	44-48	42-64	45-80

**Table 2 Thrust performance of typical magnetic layer type (M) Hall thrusters and anode layer type (A) Hall thrusters.**<sup>15,16</sup>

Thruster	SPT-50	SPT-70	SPT-100	D-38M	D-55
Species	M	M	M	A	A
Input Power, W	350	700	1350	300	1600
Thrust, mN	20	40	80	15	100
Specific impulse, s	1100	1500	1600	1500	1900
Thrust efficiency	0.35	0.45	0.50	0.37	0.60



**Figure 12. Electron current.**  $\dot{m}_{tot} = 2.73 \text{ mg/s}$ ,  $V_d = 250 \text{ V}$ .

As mentioned above,  $\dot{m}_{dif} / \dot{m}_{tot}$  increases  $I_e$  and decreases  $\eta_t$ . However, the increase of  $I_e$  appears to contribute the oscillation reduction.<sup>6</sup> As shown in Figs 6 and 8, the expansion of the anomalous diffusion range is almost coincident with the expansion of the small oscillation amplitude range (III). The relation between  $\Delta$  and  $I_e$  is shown in Fig. 14. As shown in this figure,  $\Delta$  decreases with increasing  $I_e$  in anomalous diffusion region.<sup>8</sup>

To summarize, the discharge oscillation is suppressed in exchange for the slight decrease of  $\eta_t$  because the azimuthally nonuniform propellant flows extend the anomalous diffusion range in which the tradeoff curve between  $I_e$  and  $\Delta$  is improved.

#### IV. Conclusion

The propellant was fed nonuniformly in the azimuthal direction to suppress the discharge oscillation in an anode-layer-type Hall thruster. As a result the following was found out.

1. The low oscillation amplitude range was gradually extended from the high  $B$  side with increasing  $\dot{m}_{dif} / \dot{m}_{tot}$ .
2. The operation range in which  $\Delta < 0.2$  was satisfied became wider to 42 ~ 64 mT. In this case, the ht was 39 %, which is same level as a same size of magnetic-layer-type Hall thruster.

These results indicate that the oscillation suppression was achieved in exchange for the slight decrease of  $\eta_t$ . The higher efficiency will be achieved when the channel shape is optimized.

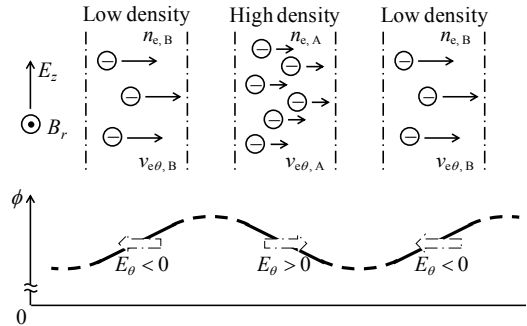


**Figure 13. Schematic of electric potential distribution created by the differential mass flow rate**

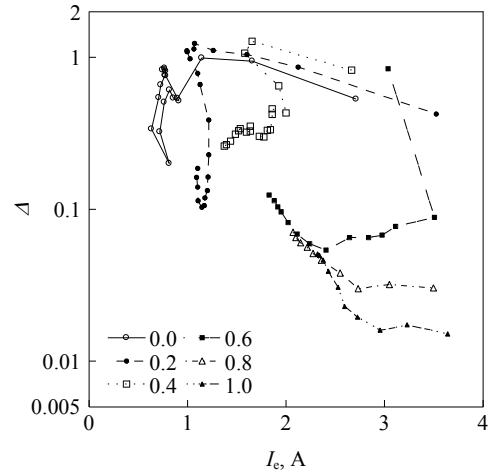


**Figure 14. The relation between  $\Delta$  and  $I_e$ .**  $\dot{m}_{tot} = 2.73 \text{ mg/s}$ ,  $V_d = 250 \text{ V}$ .

## References

- <sup>1</sup>Zhurin, V. V., Kaufman, H. R. and Robinson, R. S., "Physics of closed drift thrusters," *Plasma Sources Science and Technology*, Vol. 8, 1999, R1-R20.
- <sup>2</sup>Arakawa, Y., Komurasaki, K., Hirakawa, M., "Hall Thruster," *Journal of the Japan Society for Aeronautical and Space Sciences*, Vol. 46, 1998, pp. 146-153 (in Japanese).
- <sup>3</sup>Choueiri, E. Y., "Fundamental Difference between the Two Hall Thruster Variants," *Physics of Plasmas*, Vol. 8, 2001, pp. 5025-5033.
- <sup>4</sup>Garner, C. E., Brophy, J. R., Polk, J. E., Semenkin, S., Garkusha, V., Tverdokhlebov, S. and Marrese, C., "Experimental Evaluation of Russian Anode Layer Thrusters," AIAA Paper 94-3010, 1994.
- <sup>5</sup>Semenkin, A., Kochergin, A., Garkusha, V., Chislov, G. and Rusakov, A., "RHETT/EPDM Flight Anode Layer Thruster Development," IEPC Paper 97-106, 1997.
- <sup>6</sup>Yamamoto, N., Komurasaki, K. and Arakawa, Y., "Discharge Current Oscillation in Hall Thrusters," *Journal of Propulsion and Power*, Vol. 21, 2005, pp. 870-876.
- <sup>7</sup>Yokota, S., Yasui, S., Kumakura, K., Komurasaki, K., Arakawa, Y., "Numerical Analysis of the Sheath Structure and Discharge current Oscillation in an Anode-Layer Hall Thruster," *Journal of the Japan Society for Aeronautical and Space Sciences*, Vol. 54, 2006, pp. 39-44 (in Japanese).
- <sup>8</sup>Boeuf, J. P. and Garrigues, L., "Low frequency oscillations in a stationary plasma thruster," *Journal of Applied Physics*, Vol. 84, 1998, pp. 3541-3554.
- <sup>9</sup>Choueiri, E. Y., "Plasma oscillations in Hall thrusters," *Physics of Plasmas*, Vol. 8, 2001, pp. 1411-1426.
- <sup>10</sup>Fife, J. M., Martinez, S. M. and Szabo, J., "A numerical study of low-frequency discharge oscillations in Hall thrusters," AIAA Paper 97-3052, 1997.
- <sup>11</sup>Marchandise, F. R., Biron, J., Gambon, M., Cornu, N., Darnon, F. and Estublier, D., "The PPS-1350 qualification demonstration 7500h on ground, about 5000h in flight," IEPC Paper 2005-209, 2005.
- <sup>12</sup>Tamida, T., Nakagawa, T., Suga, I., Osuga, H., Ozaki, T. and Matsui, K., "Determining parameter sets for low-frequency-oscillation-free operation of Hall thruster," *Journal of Applied Physics*, Vol. 102, 2007, pp. 043304-1-6.
- <sup>13</sup>Nagao, N., Yokota, S., Komurasaki, K. and Arakawa, Y., "Development of a two-dimensional dual pendulum thrust stand for Hall thrusters," *Review of Scientific Instruments*, Vol. 78, 2007, pp. 115108-1-4.
- <sup>14</sup>Yamamoto, N., Komurasaki, K. and Arakawa, Y., "Condition of Stable Operation in a Hall Thruster," IEPC Paper 2003-086, 2003.
- <sup>15</sup>Kim, V., Popov, G., Arkhipov, B., Murashko, V., Gorshkov, O., Koroteyev, A., Garkusha, V., Semenkin, A. and Tverdokhlebov, S., "Electric Propulsion Activity in Russia," IEPC Paper 2001-005, 2001.
- <sup>16</sup>Semenkin, A. V., Tverdokhlebov, S. O., Garkusha, V. I., Kochergin, A. V., Chislov, G. O., Shumkin, B. V., Solodukhin, A. V. and Zakharenkov, L. E., "Operating Envelopes of Thrusters with Anode Layer," IEPC Paper 2001-013, 2001.
- <sup>17</sup>Meezan, N. B., Hargus, Jr., W. A. and Cappelli, M. A., "Anomalous electron mobility in a coaxial Hall discharge plasma," *Physical Review E*, Vol. 63, 2001, pp. 026410-1-7.
- <sup>18</sup>Hirakawa, M., Arakawa, Y., "Particle Simulation of Plasma in Electric Propulsion Thrusters," *Journal of the Japan Society for Aeronautical and Space Sciences*, Vol. 45, 1998, pp. 444-452 (in Japanese).
- <sup>19</sup>Baranov, V., Nazarenko, Y. and Petrosov, V., "Azimuthal Non-uniformities in Accelerators with Closed Electron Drift," IEPC Paper 2001-018, 2001.